

NOTICE: this is the author's version of a work that was accepted for publication in the *Journal of Molecular Biology*. Changes resulting from the publishing process, such as peer review, editing, corrections, structural formatting, and other quality control mechanisms may not be reflected in this document. Changes may have been made to this work since it was submitted for publication. A definitive version was subsequently published in *J Mol Biol* 425, 3250-3263, 9 September 2013
<http://dx.doi.org/10.1016/j.jmb.2013.06.019>

Buried and accessible surface area control intrinsic protein flexibility

Joseph A. Marsh

European Bioinformatics Institute (EMBL-EBI)

Wellcome Trust Genome Campus

Hinxton, Cambridge CB10 1SD, United Kingdom

jmarsh@ebi.ac.uk

Keywords: protein dynamics; protein structure; protein folding; monomer; solvent accessible surface area

Abbreviations used: A_{rel} , relative solvent accessible surface area; NMR, nuclear magnetic resonance; GNM, Gaussian network model; Random Coil Index, RCI; quaternary structure, QS; RMSF, root-mean-squared fluctuations

Abstract

Proteins experience a wide variety of conformational dynamics that can be crucial for facilitating their diverse functions. How is the intrinsic flexibility required for these motions encoded in their three-dimensional structures? Here, the overall flexibility of a protein is demonstrated to be tightly coupled to the total amount of surface area buried within its fold. A simple proxy for this, the relative solvent accessible surface area (A_{rel}), therefore shows excellent agreement with independent measures of global protein flexibility derived from various experimental and computational methods. Application of A_{rel} on a large scale demonstrates its utility by revealing unique sequence and structural properties associated with intrinsic flexibility. In particular, flexibility as measured by A_{rel} shows little correspondence with intrinsic disorder, but instead tends to be associated with multiple domains and increased α -helical structure. Furthermore, the apparent flexibility of monomeric proteins is found to be useful for identifying quaternary structure errors in published crystal structures. There is also a strong tendency for the crystal structures of more flexible proteins to be solved to lower resolutions. Finally, local solvent accessibility is shown to be a primary determinant of local residue flexibility. Overall this work provides both fundamental mechanistic insight into the origin of protein flexibility and a simple, practical method for predicting flexibility from protein structures.

Introduction

Proteins are intrinsically flexible, dynamic molecules. Although the structure-function insight obtained from the tens of thousands of X-ray crystal structures determined to date has demonstrated the tremendous utility of simple single-conformation models, it has long been clear, from the basic principles of statistical thermodynamics, that an ensemble representation would be required to fully describe a protein in solution. That is, rather than adopting unique structures, proteins can be considered as ensembles of multiple distinct conformers. A large body of experimental, theoretical and computational work now supports the importance of this energy landscape paradigm¹⁻³.

Although the ensemble view of protein structure is now firmly established, much progress is currently being made in characterizing the diverse ways that proteins populate the energy landscape. For many proteins, the conformational fluctuations are small and the classical representation of proteins as single unique structures is adequate for most practical purposes. Furthermore, the very fact that many proteins can be crystallized, and that those crystals are densely packed⁴, provides strong justification for the approximation of many proteins as rigid solids. However, beyond this, it is clear that proteins undergo a wide range of motions that can be important for their functions. These can involve relatively minor backbone or side-chain dynamics or larger scale movements of secondary structural elements or domains⁵. In some cases, proteins can even be intrinsically disordered, *i.e.* partially or completely unfolded in solution⁶⁻⁸, in which case the ensemble representation must cover a vast range of conformational space^{9,10}. Given this structural and dynamic diversity, protein flexibility can be best considered on a continuum, with rigid, globular proteins at one extreme and intrinsically disordered proteins at the other¹¹⁻¹³.

We recently introduced a simple parameter, the relative solvent accessible surface area (A_{rel}), which describes the amount of surface area a protein exposes to solution (and, conversely, how little it buries intramolecularly) compared to what is expected given its molecular weight. A_{rel} was shown to have great utility for predicting the magnitude of conformational changes that occur upon binding from the structures of protein complexes, allowing the demonstration that large conformational changes

are extremely common¹⁴. This work also hinted of a close relationship between A_{rel} and protein flexibility, implying a tight correspondence between the intrinsic flexibility of proteins in their unbound states and their binding-induced conformational changes.

Here, the theoretical basis for a relationship between buried and accessible surface area and intrinsic protein flexibility is first discussed, and then validated by demonstrating strong correlations between A_{rel} and various measures of flexibility calculated from normal mode analysis, NMR ensemble models, molecular dynamics simulations and NMR chemical shifts. This enables analyses of the associations between intrinsic flexibility and various protein properties, including domain structure, amino acid composition, secondary structure, quaternary structure and crystal-structure resolution. Finally, the relationship between solvent accessibility and local flexibility is investigated.

Results and Discussion

Origins of the relations between molecular weight, solvent accessible surface area and intrinsic flexibility

As the crystal structures of an increasing number of proteins were determined in the 1970s and 1980s, an interesting phenomenon was noted: when the solvent accessible surface areas of proteins was plotted against their molecular weights, a very tight correspondence was observed¹⁵⁻¹⁷. This still holds today with the large number of crystal structures that have now been determined, as shown in Figure 1A. From this plot, the expected solvent accessible surface area for a folded, crystallizable, monomeric protein ($A_{monomer}$) of molecular weight M can be fit:

$$A_{monomer} = 4.44 M^{0.770} \quad (1)$$

At first glance, this relationship might be attributed to a simple geometric phenomenon in which surface area should scale with an exponent of 2/3 with respect to volume^{16,17}. In fact, given the difference between molecular surface and solvent accessible surface area (*i.e.* the presence of a solvent layer), an exponent of slightly less than 2/3 might be expected¹⁵. However, as is seen here and noted previously^{15,18}, an exponent considerably higher than 2/3 provides the best fit. One simple interpretation of this is that larger proteins tend to adopt more extended

conformations, burying less surface area per residue than if they adopted a constant shape with increasing size. Similarly, it has been suggested that bigger proteins are less densely packed^{19,20}. Finally, an energetic explanation has been proposed: since protein folding is driven by the burial of surface area in order to compensate for the massive conformational entropy of the unfolded state^{21–23}, Equation 1 is influenced by this tendency to bury surface area in proportion to unfolded-state entropy, which in turn is proportional to molecular weight¹⁸.

Regardless of its fundamental origin, one can easily accept Equation 1 as an empirical relationship describing what is expected for a typical monomeric, crystallizable protein of a given molecular weight. We recently showed that the relative solvent accessible surface area, A_{rel} , defined as the observed solvent accessible surface area, $A_{observed}$, divided by the expected value, $A_{monomer}$, could be extremely useful for understanding the changes in conformation that a protein undergoes upon complex formation¹⁴:

$$A_{rel} = \frac{A_{observed}}{A_{monomer}} \quad (2)$$

Deviations from the idealized $A_{monomer}$ (*i.e.* A_{rel} values > 1) for both monomeric proteins and bound subunits were found to correlate with the magnitude of conformational changes that occur upon binding¹⁴. Interestingly, the A_{rel} values of a limited set of monomeric proteins were found to correlate with their flexibilities derived from normal mode analysis. Therefore, the correspondence between free-state A_{rel} values and conformational changes could be explained if increasing flexibility in the unbound state were associated with larger binding-induced conformational changes. Roughly speaking, we found that an A_{rel} value of 1.2 tends to correspond to a very large conformational change upon complex formation ($> 5 \text{ \AA}$ root-mean squared deviation between free and bound states). Given that a precision on the order of 50-100 \AA^2 is expected for solvent accessible surface area calculations²⁴, A_{rel} values can be expected to have a precision of 0.005-0.01 for a typical folded protein with $A_{observed}$ of 10^4 \AA^2 .

Why would solvent accessible surface area be related to intrinsic flexibility? Insight into this can be obtained by considering the relationship with molecular weight shown in Figure 1A. Proteins with high A_{rel} values expose more surface area than

expected for typical folded proteins and thus, crucially, bury less surface area intramolecularly within their folds. Since the burial of surface area is the primary driving force that overcomes the huge conformational entropy of the unfolded state²², proteins with higher A_{rel} values should therefore retain greater conformational entropy and be more flexible. On the other hand, proteins with lower A_{rel} values bury more surface within their folded cores and should thus be more rigid. This concept is illustrated in Figure 1B where the structures and solvent accessibilities of several monomeric proteins are shown along with their A_{rel} values.

This relationship between solvent accessible surface area and protein flexibility becomes even clearer if one assumes a constant relationship between the amount of surface area buried and the energy of folding. While proteins are of course heteropolymers comprised of chemically different amino acids, the mean hydrophobicity of accessible and buried surface area is fairly similar from one protein to another¹⁵. Moreover, the difference in energetic contribution between buried hydrophobic and hydrophilic surface area should be minimal, assuming that buried polar residues are hydrogen bonded^{25–28}. Notably, uniform surface area approaches have been found by some to be much preferable to empirical weighting schemes²⁹ and have recently shown remarkable agreement with experiments when used to predict protein complex assembly pathways^{30,31}. Therefore, by assuming constant surface area, the difference between $A_{observed}$ and $A_{monomer}$ can be directly related to the difference in conformational entropy with respect to the idealized folded state from Equation 1, and could even be converted into approximate energetic terms, for instance by assuming ~0.1 kJ/mol of conformational entropy per additional \AA^2 exposed compared to the reference state²⁵. A_{rel} therefore effectively represents a simple proxy for this difference in conformational entropy, normalized to protein size, explaining why it would be closely related to intrinsic protein flexibility.

A_{rel} predicts global measures of intrinsic flexibility

The above suggests that A_{rel} , which functions essentially as a measure of how little surface area a protein buries within its fold, should be related to flexibility. How strong is this relationship, and could it be of practical utility? Here this is investigated in detail through large-scale comparisons of monomer A_{rel} values to multiple independent probes of intrinsic protein flexibility. Although various definitions of

flexibility have been used in different contexts, here we are considering intrinsic flexibility in a general sense, as a scalar quantity describing the magnitude of conformational dynamics that a protein will experience isolated in solution. Each flexibility measure used here is very different, being based upon different simulation methods or experimental data, but they are all reflective of intrinsic flexibility in the sense that they quantify the overall extent of protein motions.

A non-redundant set of 6565 monomeric protein crystal structures was first compiled, as well as a subset of 907 high-confidence monomers that have been filtered using much stricter criteria. The high-confidence monomers were used to fit the relationship in Equation 1 (Figure 1A). Figure 1C shows the distribution of A_{rel} values for both sets. A smooth distribution is observed with a peak at 1.0, suggesting that A_{rel} represents a continuous phenomenon with a range of possible values, consistent with the continuum view of protein dynamics. The asymmetric nature of the distribution implies that there are fairly tight constraints on how much surface area a protein can possibly bury intramolecularly (with no observed $A_{\text{rel}} < 0.8$) and looser restrictions on how much surface area a crystallizable monomer can expose (with a few instances of $A_{\text{rel}} > 1.5$).

Normal mode analysis provides a fast and simple way to probe the intrinsic flexibility and dynamics of proteins of known structure. Excellent agreement has been obtained between normal mode analysis applied to simple backbone-only models of various proteins and the intrinsic dynamics and conformational changes observed experimentally or in molecular dynamics simulations^{32–36}. In this study, the Gaussian network model (GNM)³⁷ was used for large-scale normal mode analysis. Figure 2A plots the flexibility values calculated with GNM (*i.e.* the mean amplitudes of their normal modes) against A_{rel} for all 6565 monomeric crystal structures. Overall, a strong correspondence is observed (Pearson correlation coefficient $r = 0.78$), confirming the effectiveness of A_{rel} as a proxy for intrinsic flexibility derived from normal mode analysis. Notably, the correlation with the large dataset used here is very similar to what was seen previously with only 60 proteins ($r = 0.76$)¹⁴, using a different method of normal mode analysis (elastic network model^{38,39}).

Models of protein structures calculated from NMR data generally contain multiple distinct conformations. While the structural heterogeneity among different ensemble members arises from both the intrinsic dynamics of a protein and of possible

uncertainty reflecting an insufficient number of experimental restraints, NMR ensemble models generally provide reasonable, albeit imperfect, representations of the solution dynamics^{40–43}. The NMR ensemble models used in this study came from the RECOORD database and have all been recalculated using a uniform protocol⁴⁴, thus avoiding some of the variation between models that arises due to methodological differences. Figure 2B plots the root-mean-squared fluctuations (RMSF) for 454 non-redundant NMR models against their A_{rel} values. Overall, there is a strong correlation between A_{rel} and RMSF ($r = 0.82$), demonstrating that A_{rel} is highly reflective of the fluctuations within an NMR model.

Molecular dynamics simulations provide another way to characterize the intrinsic flexibility and dynamics of proteins in detail. This study utilized a large set of 10 ns trajectories from the MoDEL database, which contains pre-calculated parameters describing the global flexibility of each protein⁴⁵. Figure 2C compares A_{rel} to the Lindemann index calculated from the molecular dynamics trajectories of 491 non-redundant monomeric proteins. This parameter provides a measure of atomic-level disorder, and can thus be used as a descriptor of the liquid-like or solid-like character of a protein⁴⁶. The correlation is strong ($r = 0.77$) confirming that A_{rel} shows major overlap with flexibility derived from molecular dynamics simulations. Likewise, an alternate measure of flexibility available in MoDEL, the mean variance of C α atoms, shows a similar correlation of 0.73 with A_{rel} (Figure S1).

The Random Coil Index (RCI) is based upon NMR chemical shifts and provides a local measure of backbone flexibility⁴⁷. Figure 2D plots the global RCI values, averaged over all residues, against A_{rel} values calculated from 185 non-redundant NMR models. The correlation is good ($r = 0.71$), although slightly lower than the other examined flexibility measures. Importantly, RCI is directly calculated from experimental chemical shifts, which were not used in the NMR model calculations, and is thus independent of the structural models used to calculate A_{rel} .

Together, the above results demonstrate that the overall flexibility of monomeric proteins is strongly determined by the total amount of surface area buried within their folds, and thus the simple-to-calculate A_{rel} parameter is highly predictive of various flexibility measures. Table S1 shows how those different measures correlate with each other. For example, while the Lindemann index shows a correlation of 0.77 with A_{rel} values, it has markedly lower correlations with RMSF (0.70), RCI

(0.57) and GNM (0.68). Strikingly, the A_{rel} values correlate with all four measures of intrinsic flexibility as well as, or better than, those measures do with each other. Furthermore, it was also found that the choice of monomer set used for fitting Equation 1 had little effect on the predictive ability of A_{rel} (Table S2).

Flexibility depends on protein length and number of domains

A_{rel} , by definition, is essentially normalized to protein length ($r = 0.999$ between number of residues and molecular weight in the full dataset), and reflects the flexibility with respect to an idealized state expected for a protein of a given molecular weight. However, there does appear to be some length dependence to protein flexibility, as there is a slight correlation between A_{rel} and chain length ($r = 0.17$). One possibility is that this is related to the number of protein domains, as the presence of multiple domains can facilitate considerable inter-domain motions^{5,48}. Indeed, the correlation between A_{rel} and number of domains is much stronger ($r = 0.31$), while the correlation with chain length largely disappears if one considers only single-domain proteins ($r = 0.07$). Figure 3 demonstrates the strong tendency for mean A_{rel} values to increase with an increasing number of domains.

Could the motions facilitated by the presence of multiple domains be a primary determinant of the relationship observed between A_{rel} and other measures of flexibility? Table S3 shows that this is not the case by breaking down the analyses by single- and two-domain proteins, and showing that the strong correlations are still preserved. Thus A_{rel} clearly captures much more of the broad spectrum of protein flexibility than just inter-domain motions.

The influence of multidomain proteins on the fit in Figure 1A used to derive Equation 1 was also considered. If multidomain proteins are excluded, Equation 1 changes to $5.82M^{0.74}$. This suggests that, unexpectedly, the approximation of proteins adopting relatively constant shapes becomes slightly more accurate when considering only single-domain proteins, as the exponent is closer to $2/3$. However, most importantly for our purposes, the correlations with different measures of intrinsic flexibility change very little if this form of the equation is used to calculate A_{rel} (Table S2).

Flexible proteins are characterized by unique sequence and secondary structure properties

To what extent is the propensity for protein flexibility reflected in amino acid composition? To assess this, the Pearson correlation coefficient (r) was calculated between the fractional content of each of the 20 standard amino acids and the A_{rel} values of monomeric crystal structures (Figure 4A). Thus amino acids that tend to be associated with higher- A_{rel} , more flexible proteins will have higher r values, while those associated with more rigid proteins will have negative r . Each amino acid is coloured by its type (hydrophobic, charged, polar and glycine), which allows some interesting trends to be immediately noted. Charged amino acids, with the exception of aspartate, have a strong association with increased flexibility. On the other hand, polar amino acids are generally associated with lower flexibility. Interestingly, and somewhat surprisingly, hydrophobic amino acids tend to be intermediate between polar and charged residues. Finally, glycine shows the strongest negative correlation with A_{rel} . Very similar sequence trends are observed if alternate measures of flexibility are considered (Figure S2A).

Some correspondence between the sequence determinants of intrinsic disorder and intrinsic flexibility as measured by A_{rel} might be expected. For instance, protein complex subunits predicted to be disordered have been found to have much higher A_{rel} values than those predicted to fold^{14,49}. Contact density, which is closely related to buried surface area, has also been identified as an important parameter for predicting intrinsically disordered regions^{50–52}. Furthermore, regions of proteins predicted to be disordered yet observed in crystal structures tend to undergo larger conformational changes⁵³. Therefore, it is noteworthy that the association between A_{rel} and charged residues is analogous to the previous observations that net charge is the primary determinant of expandedness in intrinsically disordered proteins^{54–56}. Beyond this, however, there appears to be little further similarity with the known sequence determinants of disorder^{7,8}. For example, glycine is strongly associated with intrinsic disorder yet here inversely correlates with A_{rel} . Moreover, leucine is relatively rare in disordered proteins, yet here shows one of the strongest correlations with increased flexibility. Table S4 shows there are only weak correlations between the A_{rel} values of monomeric proteins and multiple sequence-based disorder predictions, suggesting that, for the most part, intrinsic disorder and

monomer flexibility as manifested by A_{rel} are reflective of different regions of the protein dynamics continuum.

In contrast to intrinsic disorder, there does appear to be a clear association between A_{rel} and the secondary structure propensities of different amino acids. In particular, glutamate, leucine and lysine have strong α -helical propensities, while glycine, tyrosine and asparagine are helix destabilizing⁶². Therefore, given this apparent correspondence between flexibility and secondary structure propensities, the A_{rel} values of monomer crystal structures from different SCOP classes⁵⁸ were compared (Figure 4B). Consistent with the sequence trend, this analysis reveals that all- α proteins are the most flexible (mean $A_{rel} = 1.050$) and all- β proteins the most rigid (mean $A_{rel} = 0.984$, $P < 2.2 \times 10^{-16}$, Wilcoxon test). The mixed classes ($\alpha+\beta$ and α/β) have A_{rel} values intermediate to α and β , although α/β and β are nearly equal. This tendency for α proteins to be more flexible than β proteins maintained when alternate measures of flexibility are considered instead of A_{rel} (Figure S2B). Furthermore, the sequence trends and correlations between A_{rel} and different measures of flexibility are preserved when split by structural class, demonstrating that they are largely independent of secondary structure (Figure S3 and Table S5).

What is the origin of this difference in flexibility between α and β proteins? One explanation is that β -strands are more often associated with changes in the direction of the polypeptide chain. Thus one can easily imagine why β proteins would tend to form more compact, low- A_{rel} structures that bury more surface area within their folds. In contrast, α -helices only require the chain to go in a single direction, so more extended, high- A_{rel} structures can be facilitated by the presence of helical structure. It is also interesting that many of the most compact, low- A_{rel} structures contain a mixture of both α and β structure, as for example seen in the TIM barrel β -mannanase shown in Figure 1B (PDB ID: 1BQC); in these cases the combination of α and β structure may facilitate their highly pseudosymmetrical folds. Interestingly, α/β proteins were recently shown to be the most compact structural class and to exhibit the slowest folding rates, which was attributed to the fact that they were able to adopt the most spherical structures⁵⁹⁻⁶¹. This helps to explain how these proteins are able to so efficiently bury surface area and adopt overall rigid conformations. In light of these observations, it is interesting to note the recent finding that proteins

with β structure tend to have slightly different A_s vs. molecular weight relationships (*i.e.* Equation 1) than all- α proteins⁶³, which could imply that larger β proteins tend to be relatively more flexible than larger α proteins, in comparison with smaller proteins.

These results could also possibly be related to the strong relationship between low A_{rel} values and polar residues, if the requirement for these side chains to form intramolecular hydrogen bonds is associated with changes in backbone direction, *e.g.* for stabilizing turns or long-range β -strand contacts⁵⁷. Similarly, the strong association between glycine and rigidity could be related to its favourability for forming type-II β -turns. Thus, while the vast Ramachandran space available to glycine is often associated with local flexibility, the results here suggest that this also gives it the ability to facilitate globally rigid structures that can effectively bury surface area and stabilize their folds.

Quaternary structure errors are associated with high apparent flexibility

Careful examination of the unit cells of monomeric crystal structures with high A_{rel} values suggested that some of these were actually homo-oligomeric, with the monomeric biological unit likely being assigned in error. For example, the structure of TrmD (PDB ID: 1P9P) is shown in Figure 5A. This structure has an author-assigned monomeric biological unit with a high A_{rel} value (1.29), yet it has been manually annotated as a dimer in the PiQSi database of manually curated quaternary structure (QS)⁶⁴ and is also predicted to be dimer by PISA⁶⁵.

To investigate the relationship between apparent flexibility and the propensity for QS misassignments, correctly and incorrectly assigned monomers were identified from PiQSi. On average, confirmed monomers tend to have lower A_{rel} values (1.01) than those assigned in error (1.08, $P = 2 \times 10^{-6}$, Wilcoxon test), thus demonstrating that incorrectly assigned monomers are associated with greater apparent flexibility. Figure 5B shows the frequency of QS errors for proteins grouped by A_{rel} values. Notably, there is a strong tendency for the frequency of QS errors to increase with higher A_{rel} . Thus while A_{rel} alone would not be able to absolutely identify QS errors, this plot can be used to roughly assess the likelihood that an apparently monomeric protein with a given A_{rel} value is the result of a QS misassignment. This could

potentially be of considerable use in QS-prediction algorithms, which incorporate many factors.

Intrinsic flexibility is a major determinant of crystal structure resolution

Decades of experience have shown that flexible proteins are generally difficult to crystallize. Therefore, it is natural to ask whether there might be a relationship between the intrinsic flexibility of a protein and the resolution of its crystal structure. Figure 6A plots the mean A_{rel} values for monomeric crystal structures grouped by resolution. Interestingly, there is a marked tendency for proteins with lower resolution crystal structures to be more flexible. For instance, very high-resolution monomers ($< 1 \text{ \AA}$) have a mean A_{rel} of 0.97, compared to 1.19 for those of low resolution ($\geq 3.5 \text{ \AA}$) ($P = 4 \times 10^{-8}$, Wilcoxon test). This relationship is preserved even when only crystal structures with no disordered residues are considered and is also confirmed with different measures of flexibility (Figure S4).

An interesting consequence of this result is that, as protein crystallography has experienced methodological improvements, the ability to solve lower resolution crystal structures and thus probe more flexible regions of protein conformational space has improved. Figure 6B shows the mean A_{rel} values of monomeric crystal structures solved over time. A clear tendency is observed for more recently determined crystal structures to represent more flexible proteins. Therefore, as experimental and computational methods for modelling lower resolution crystal structures continue to improve⁶⁶, the available coverage of the protein dynamics continuum will continue to broaden.

Residue-specific A_{rel} reflects local flexibility

Since A_{rel} is based upon the total solvent accessible surface area, it therefore provides no information on local protein flexibility. However, we can easily employ a residue-specific local A_{rel} measure, defining it as the ratio of the observed solvent accessible surface area for a residue to the expected unfolded-state value for that amino acid type¹⁵. Similar approaches have been used in the past, for instance in defining buried and accessible residues⁶⁷. In addition, local solvent accessibility is known to be closely related to B factors from crystal structures^{68–70} and order parameters from NMR relaxation experiments⁷¹. Therefore, to complement the

above global analyses, local A_{rel} values have been compared to residue-specific flexibility values derived from normal mode analysis, NMR ensemble models and chemical shifts.

The distributions of Pearson correlation coefficients calculated for individual proteins between local A_{rel} values and local flexibilities calculated from different methods are shown in Figure 7A-C. Overall, mean correlations of 0.74 for GNM, 0.70 for RMSF and 0.61 for RCI are observed. Thus local A_{rel} provides fairly reasonable predictions of local flexibility for all of these methods. The origin of this relationship is the same as discussed earlier for global flexibility: proteins with lower local A_{rel} values bury more surface area, making more extensive intramolecular contacts, and are thus more motionally restricted. In effect, local A_{rel} here is functioning similarly to the simple contact models showing that flexibility is primarily determined by local contact density, thus allowing prediction of B factors, NMR order parameters^{72,73} or intrinsic disorder^{51,52}.

Conclusion

Although it has long been clear that protein flexibility is important for function, characterizing this flexibility can be difficult. Here it is shown that A_{rel} , which functions essentially as a proxy for how much surface area a protein buries within its fold, correlates remarkably well with different measures of intrinsic protein flexibility. This allows the easy assessment of protein flexibility in a quantitative manner from the large number of protein structures now available, and has revealed new insight into the relationships between protein flexibility, sequence and structure. Many more topics of inquiry remain open for future exploration, relating to diverse aspects of protein structure, function, sequence and evolution.

The major advantage of A_{rel} as a probe of protein flexibility is its simplicity. It can be quickly and easily calculated from any protein structure. Furthermore, its correlation with intrinsic flexibility arises directly from the fundamental energetics of protein folding, so its utility is not merely empirical. While treating surface area uniformly works remarkably well for many purposes, it is possible that a model considering the specific properties of a protein's surface could provide a better probe of flexibility. However, the fact that A_{rel} correlates as good or better with different measures of intrinsic flexibility than they do with each other suggests that any room for

improvement with a more complex model should be minimal.

Another potential issue relevant to this study relates to crystallographic disorder, which results in residues missing from the crystal structures. Since this study dealt primarily with structure-based measures of flexibility here, the effect of ignoring disordered residues should be small. However, in principle, disordered residues could be dealt with, either by explicit modelling⁷⁴, or by simply assigning them statistical accessibilities, with the assumption that they do not form any non-local contacts. Importantly, all trends in this study are retained when considering only high-confidence monomers with no disordered residues.

Previously, A_{rel} values of both monomeric proteins and bound subunits were used to predict protein conformational changes upon binding¹⁴. Analysis of the free/bound pairs shows a very strong correlation between the A_{rel} values of monomeric proteins and their A_{rel} values in the bound state. This suggests that, in addition to their utility for predicting conformational changes upon binding, the A_{rel} values of bound subunits are predictive of the flexibility of proteins in their free states, thus facilitating large-scale analyses of how intrinsic flexibility relates to protein complex assembly from the structures of protein complexes.

Finally, it is interesting to note that the unique amino acid properties associated with intrinsic flexibility appear to be distinct from intrinsic disorder. Given the success of intrinsic disorder predictors, it is tempting to speculate that a sequence-based predictor of flexibility could be developed using A_{rel} values as a training set. Previously B factors have been used in a similar manner to train sequence-based flexibility predictors^{75,76}, although the amino acids associated with high B factors are quite different than the sequence determinants of flexibility observed here, likely due to the differences between global and local flexibility. It is possible that the topological complexity of protein folds might inhibit a sequence-based predictor of folded protein flexibility, as compared to intrinsically disordered proteins where the amino acid composition can sometimes be more important than the specific linear sequence⁷⁷. However, the availability of a sequence-based predictor would facilitate genome-scale analyses of the relationships between protein flexibility, function and evolution.

Methods

Monomer datasets

All monomeric crystal structure biological units containing at least 30 residues were taken from Protein Data Bank on 2012-08-08, excluding backbone-only models. The set of high-confidence monomers (used for fitting the relationship in Figure 1A) included only monomers with SCOP 1.75 domain assignments⁵⁸ in order to specifically exclude structures in the classes “membrane and cell surface proteins and peptides”, “small proteins”, “coiled coil proteins”, “low resolution protein structures”, “peptides” and “designed proteins”. In addition, only proteins which had a single chain in the asymmetric unit and which were predicted to be monomeric by PISA⁶⁵ were considered. Furthermore, structures which contained $\geq 1\%$ non-protein atoms were excluded. Finally, proteins in which any non-terminal residues were missing from the crystal structure (*i.e.* disordered) were excluded.

The full crystal-structure dataset used for most of this paper also included only proteins that were predicted to be monomeric by PISA, and excluded structures which contained $\geq 10\%$ non-protein atoms. In addition, any structures containing a large number of missing, non-terminal residues (containing any stretches of > 20 missing residues, or > 50 missing residues in total) were excluded. For the dataset used in the QS-assignment analysis, the same criteria were used, except for the condition that proteins be PISA-predicted monomers.

The NMR ensemble models were taken from the RECOORD database and have all been recalculated using a uniform protocol and refined in water⁴⁴.

For all datasets, sequence redundancy filtering was performed at a level of 90% identity, after the above criteria were applied. This left 907 non-redundant proteins in the high-confidence set, 6565 in the full set, 491 with MoDEL parameters, 454 in the NMR set and 267 in the set with PiQSi QS assignments. All protein structures and relevant parameters related to these analyses are provided in Table S7.

Structural and flexibility calculations

Solvent accessible surface area

Solvent accessible surface area was calculated from each crystal structure and

each NMR model ensemble member using AREAIMOL⁷⁸. For calculating A_{rel} , the solvent accessible surface area was averaged over all NMR ensemble members. For the local A_{rel} calculations, the unfolded-state values of Miller *et al.* were used¹⁵, and values were averaged over a seven-residue window. All correlations with A_{rel} were calculated using the log of the flexibility parameters, consistent with what was done previously for conformational changes¹⁴ since this tends to give much more linear relationships.

Normal mode analysis

The Gaussian network model³⁷ was used with default parameters and considering only backbone $C\alpha$ atoms. For each protein, n normal modes are calculated with GNM for a protein with $n + 1$ residues. The flexibility of each protein was calculated as the average of the inverse eigenvalue (*i.e.* frequency, ω_i) of each normal mode (Equation 3). This value therefore represents the mean amplitude of a protein's normal modes.

$$GNM(\text{global}) = \frac{\sum_i^n \frac{1}{\omega_i}}{n} \quad (3)$$

The residue-specific flexibility for residue j is given in Equation 4, where a_{ij} is the displacement of residue j under mode i .

$$GNM(\text{local})_j = \sum_i^n \frac{a_{ij}^2}{\omega_i} \quad (4)$$

NMR models

For each NMR ensemble model, the residue-averaged RMSF was calculated according to Equation 5, where d_{ij} is the distance between each backbone $C\alpha$ atom i from conformer j and the ensemble-averaged position of that atom, m is the total number of conformers in the ensemble, and n is the total number of residues in the protein.

$$RMSF = \frac{1}{n} \sqrt{\frac{1}{m} \sum_{j=1}^m d_{ij}^2} \quad (5)$$

Molecular dynamics simulations

All parameters were taken directly from the MoDEL database and were calculated from 10 ns trajectories using AMBER8 or AMBER9 with parm99 force field and TIP3P water model⁴⁵. Because trajectories in MoDEL were only calculated for a limited subset of all available monomeric proteins, a separate 90% sequence identity redundancy filtering was performed with these proteins.

NMR chemical shifts

The BioMagResBank⁷⁹ was searched for sets of chemical shifts that corresponded to our non-redundant NMR models. In total, chemical shifts were available for 185 of these proteins. The Random Coil Index (RCI) values were then calculated from these chemical shifts using the RCI web server⁴⁷. For the global RCI measure, the residue-specific values were averaged over all positions.

Acknowledgements

I thank Tim Meyer from providing data from MoDEL and Sarah Teichmann, Julie Forman-Kay, Tina Perica and A.J Venkatakrishnan for valuable comments on the manuscript. This work was supported by a Long-term Fellowship from the Human Frontier Science Program.

References

1. Henzler-Wildman, K. & Kern, D. (2007). Dynamic personalities of proteins. *Nature* **450**, 964–972
2. Frauenfelder, H., Sligar, S.G. & Wolynes, P.G. (1991). The energy landscapes and motions of proteins. *Science* **254**, 1598–1603
3. Tsai, C.J., Kumar, S., Ma, B. & Nussinov, R. (1999). Folding funnels, binding funnels, and protein function. *Protein Sci* **8**, 1181–1190
4. Tsai, J., Taylor, R., Chothia, C. & Gerstein, M. (1999). The packing density in proteins: standard radii and volumes. *J. Mol. Biol.* **290**, 253–266
5. Gerstein, M., Lesk, A.M. & Chothia, C. (1994). Structural mechanisms for domain movements in proteins. *Biochemistry* **33**, 6739–6749
6. Wright, P.E. & Dyson, H.J. (1999). Intrinsically unstructured proteins: re-

- assessing the protein structure-function paradigm. *J. Mol. Biol* **293**, 321–331
7. Uversky, V.N., Gillespie, J.R. & Fink, A.L. (2000). Why are “natively unfolded” proteins unstructured under physiologic conditions? *Proteins* **41**, 415–427
 8. Dunker, A.K., Lawson, J.D., Brown, C.J., Williams, R.M., Romero, P., Oh, J.S., Oldfield, C.J., Campen, A.M., Ratliff, C.M., Hipps, K.W., Ausio, J., Nissen, M.S., Reeves, R., Kang, C., Kissinger, C.R., Bailey, R.W., Griswold, M.D., Chiu, W., Garner, E.C. & Obradovic, Z. (2001). Intrinsically disordered protein. *J. Mol. Graph. Model* **19**, 26–59
 9. Marsh, J.A. & Forman-Kay, J.D. (2012). Ensemble modeling of protein disordered states: Experimental restraint contributions and validation. *Proteins* **80**, 556–572
 10. Schneider, R., Huang, J., Yao, M., Communie, G., Ozenne, V., Mollica, L., Salmon, L., Jensen, M.R. & Blackledge, M. (2012). Towards a robust description of intrinsic protein disorder using nuclear magnetic resonance spectroscopy. *Mol Biosyst* **8**, 58–68
 11. Fisher, C.K. & Stultz, C.M. (2011). Protein structure along the order–disorder continuum. *J Am Chem Soc* **133**, 10022–10025
 12. Marsh, J.A., Teichmann, S.A. & Forman-Kay, J.D. (2012). Probing the diverse landscape of protein flexibility and binding. *Curr. Opin. Struct. Biol* **22**, 643–650
 13. Hensen, U., Meyer, T., Haas, J., Rex, R., Vriend, G. & Grubmüller, H. (2012). Exploring protein dynamics space: the dynasome as the missing link between protein structure and function. *PLoS ONE* **7**, e33931
 14. Marsh, J.A. & Teichmann, S.A. (2011). Relative solvent accessible surface area predicts protein conformational changes upon binding. *Structure* **19**, 859–867
 15. Miller, S., Janin, J., Lesk, A.M. & Chothia, C. (1987). Interior and surface of monomeric proteins. *J. Mol. Biol* **196**, 641–656
 16. Teller, D.C. (1976). Accessible area, packing volumes and interaction surfaces of globular proteins. *Nature* **260**, 729–731
 17. Janin, J. (1976). Surface area of globular proteins. *J. Mol. Biol* **105**, 13–14
 18. Miller, S., Lesk, A.M., Janin, J. & Chothia, C. (1987). The accessible surface area and stability of oligomeric proteins. *Nature* **328**, 834–836
 19. Fischer, H., Polikarpov, I. & Craievich, A.F. (2004). Average protein density is a molecular-weight-dependent function. *Protein Sci* **13**, 2825–2828
 20. Liang, J. & Dill, K.A. (2001). Are proteins well-packed? *Biophys. J* **81**, 751–766
 21. Kauzmann, W. (1959). Some factors in the interpretation of protein denaturation. *Adv. Protein Chem.* **14**, 1–63
 22. Chothia, C. (1975). Structural invariants in protein folding. *Nature* **254**, 304–308
 23. Dill, K.A. & MacCallum, J.L. (2012). The protein-folding problem, 50 years on. *Science* **338**, 1042–1046
 24. Novotny, M., Seibert, M. & Kleywegt, G.J. (2007). On the precision of calculated solvent-accessible surface areas. *Acta Crystallogr. D Biol. Crystallogr.* **63**, 270–274
 25. Chothia, C. (1974). Hydrophobic bonding and accessible surface area in proteins. *Nature* **248**, 338–339
 26. Loladze, V.V., Ermolenko, D.N. & Makhatadze, G.I. (2002). Thermodynamic consequences of burial of polar and non-polar amino acid residues in the protein interior. *J. Mol. Biol.* **320**, 343–357
 27. McDonald, I.K. & Thornton, J.M. (1994). Satisfying hydrogen bonding potential in proteins. *J. Mol. Biol.* **238**, 777–793
 28. Takano, K., Yamagata, Y. & Yutani, K. (2001). Contribution of polar groups in the

- interior of a protein to the conformational stability. *Biochemistry* **40**, 4853–4858
29. Eyal, E., Najmanovich, R., McConkey, B.J., Edelman, M. & Sobolev, V. (2004). Importance of solvent accessibility and contact surfaces in modeling side-chain conformations in proteins. *J Comput Chem* **25**, 712–724
 30. Levy, E.D., Erba, E.B., Robinson, C.V. & Teichmann, S.A. (2008). Assembly reflects evolution of protein complexes. *Nature* **453**, 1262–1265
 31. Marsh, J.A., Hernández, H., Hall, Z., Ahnert, S., Perica, T., Robinson, C.V. & Teichmann, S.A. (2013). Protein complexes are under evolutionary selection to assemble via ordered pathways. *Cell* **153**, 461–470
 32. Ahmed, A., Villinger, S. & Gohlke, H. (2010). Large-scale comparison of protein essential dynamics from molecular dynamics simulations and coarse-grained normal mode analyses. *Proteins* **78**, 3341–3352
 33. Bahar, I. & Rader, A.J. (2005). Coarse-grained normal mode analysis in structural biology. *Curr. Opin. Struct. Biol.* **15**, 586–592
 34. Rueda, M., Chacón, P. & Orozco, M. (2007). Thorough validation of protein normal mode analysis: a comparative study with essential dynamics. *Structure* **15**, 565–575
 35. Tama, F. & Sanejouand, Y.H. (2001). Conformational change of proteins arising from normal mode calculations. *Protein Eng.* **14**, 1–6
 36. Mendez, R. & Bastolla, U. (2010). Torsional network model: normal modes in torsion angle space better correlate with conformation changes in proteins. *Phys. Rev. Lett.* **104**, 228103
 37. Bahar, I., Wallqvist, A., Covell, D.G. & Jernigan, R.L. (1998). Correlation between native-state hydrogen exchange and cooperative residue fluctuations from a simple model. *Biochemistry* **37**, 1067–1075
 38. Suhre, K. & Sanejouand, Y.-H. (2004). Elnemo: a normal mode web server for protein movement analysis and the generation of templates for molecular replacement. *Nucleic Acids Research* **32**, W610–W614
 39. Dobbins, S.E., Lesk, V.I. & Sternberg, M.J.E. (2008). Insights into protein flexibility: The relationship between normal modes and conformational change upon protein-protein docking. *Proc. Natl. Acad. Sci. U.S.A* **105**, 10390–10395
 40. Yang, L.-W., Eyal, E., Chennubhotla, C., Jee, J., Gronenborn, A.M. & Bahar, I. (2007). Insights into equilibrium dynamics of proteins from comparison of NMR and X-ray data with computational predictions. *Structure* **15**, 741–749
 41. Abseher, R., Horstink, L., Hilbers, C.W. & Nilges, M. (1998). Essential spaces defined by NMR structure ensembles and molecular dynamics simulation show significant overlap. *Proteins* **31**, 370–382
 42. Philippopoulos, M. & Lim, C. (1999). Exploring the dynamic information content of a protein NMR structure: Comparison of a molecular dynamics simulation with the NMR and X-ray structures of Escherichia coli ribonuclease HI. *Proteins* **36**, 87–110
 43. Andersen, C.A.F., Palmer, A.G., Brunak, S. & Rost, B. (2002). Continuum secondary structure captures protein flexibility. *Structure* **10**, 175–184
 44. Nederveen, A.J., Doreleijers, J.F., Vranken, W., Miller, Z., Spronk, C.A.E.M., Nabuurs, S.B., Güntert, P., Livny, M., Markley, J.L., Nilges, M., Ulrich, E.L., Kaptein, R. & Bonvin, A.M.J.J. (2005). RECOORD: A recalculated coordinate database of 500+ proteins from the PDB using restraints from the BioMagResBank. *Proteins* **59**, 662–672
 45. Meyer, T., D'Abbramo, M., Hospital, A., Rueda, M., Ferrer-Costa, C., Pérez, A., Carrillo, O., Camps, J., Fenollosa, C., Repchevsky, D., Gelpí, J.L. & Orozco, M.

- (2010). MoDEL (Molecular Dynamics Extended Library): a database of atomistic molecular dynamics trajectories. *Structure* **18**, 1399–1409
46. Zhou, Y., Vitkup, D. & Karplus, M. (1999). Native proteins are surface-molten solids: application of the lindemann criterion for the solid versus liquid state. *J Mol Biol* **285**, 1371–1375
 47. Berjanskii, M.V. & Wishart, D.S. (2005). A simple method to predict protein flexibility using secondary chemical shifts. *J. Am. Chem. Soc.* **127**, 14970–14971
 48. Bernado, P., Modig, K., Grela, P., Svergun, D.I., Tchorzewski, M., Pons, M. & Akke, M. (2010). Structure and Dynamics of Ribosomal Protein L12: An Ensemble Model Based on SAXS and NMR Relaxation. *Biophys J* **98**, 2374–2382
 49. Gunasekaran, K., Tsai, C.-J. & Nussinov, R. (2004). Analysis of ordered and disordered protein complexes reveals structural features discriminating between stable and unstable monomers. *J. Mol. Biol* **341**, 1327–1341
 50. Dosztányi, Z., Csizmók, V., Tompa, P. & Simon, I. (2005). The pairwise energy content estimated from amino acid composition discriminates between folded and intrinsically unstructured proteins. *J. Mol. Biol* **347**, 827–839
 51. Garbuzynskiy, S.O., Lobanov, M.Y. & Galzitskaya, O.V. (2004). To be folded or to be unfolded? *Protein Sci.* **13**, 2871–2877
 52. Galzitskaya, O.V., Garbuzynskiy, S.O. & Lobanov, M.Y. (2006). Prediction of amyloidogenic and disordered regions in protein chains. *PLoS Comput. Biol.* **2**, e177
 53. Bhardwaj, N. & Gerstein, M. (2009). Relating protein conformational changes to packing efficiency and disorder. *Protein Sci* **18**, 1230–1240
 54. Mao, A.H., Crick, S.L., Vitalis, A., Chicoine, C.L. & Pappu, R.V. (2010). Net charge per residue modulates conformational ensembles of intrinsically disordered proteins. *Proc. Natl. Acad. Sci. U.S.A.* **107**, 8183–8188
 55. Marsh, J.A. & Forman-Kay, J.D. (2010). Sequence determinants of compaction in intrinsically disordered proteins. *Biophys. J* **98**, 2383–2390
 56. Müller-Spáth, S., Soranno, A., Hirschfeld, V., Hofmann, H., Rügger, S., Reymond, L., Nettels, D. & Schuler, B. (2010). Charge interactions can dominate the dimensions of intrinsically disordered proteins. *Proc. Natl. Acad. Sci. U.S.A.* **107**, 14609–14614
 57. Levitt, M. (1978). Conformational preferences of amino acids in globular proteins. *Biochemistry* **17**, 4277–4285
 58. Murzin, A.G., Brenner, S.E., Hubbard, T. & Chothia, C. (1995). SCOP: a structural classification of proteins database for the investigation of sequences and structures. *J. Mol. Biol* **247**, 536–540
 59. Galzitskaya, O.V., Reifsnnyder, D.C., Bogatyreva, N.S., Ivankov, D.N. & Garbuzynskiy, S.O. (2008). More compact protein globules exhibit slower folding rates. *Proteins* **70**, 329–332
 60. Ivankov, D.N., Bogatyreva, N.S., Lobanov, M.Y. & Galzitskaya, O.V. (2009). Coupling between properties of the protein shape and the rate of protein folding. *PLoS ONE* **4**, e6476
 61. Lobanov, M.I., Bogatyreva, N.S. & Galzitskaia, O.V. (2008). [Radius of gyration is indicator of compactness of protein structure]. *Mol. Biol. (Mosk.)* **42**, 701–706
 62. Bordo, D. & Argos, P. (1994). The role of side-chain hydrogen bonds in the formation and stabilization of secondary structure in soluble proteins. *J. Mol. Biol.* **243**, 504–519
 63. Glyakina, A.V., Bogatyreva, N.S. & Galzitskaya, O.V. (2011). Accessible surfaces

- of beta proteins increase with increasing protein molecular mass more rapidly than those of other proteins. *PLoS ONE* **6**, e28464
64. Levy, E.D. (2007). PiQSi: protein quaternary structure investigation. *Structure* **15**, 1364–1367
 65. Krissinel, E. & Henrick, K. (2007). Inference of macromolecular assemblies from crystalline state. *J. Mol. Biol* **372**, 774–797
 66. Schröder, G.F., Levitt, M. & Brunger, A.T. (2010). Super-resolution biomolecular crystallography with low-resolution data. *Nature* **464**, 1218–1222
 67. Levy, E.D. (2010). A simple definition of structural regions in proteins and its use in analyzing interface evolution. *J. Mol. Biol.* **403**, 660–670
 68. Carugo, O. & Argos, P. (1997). Correlation between side chain mobility and conformation in protein structures. *Protein Eng.* **10**, 777–787
 69. Sheriff, S., Hendrickson, W.A., Stenkamp, R.E., Sieker, L.C. & Jensen, L.H. (1985). Influence of solvent accessibility and intermolecular contacts on atomic mobilities in hemerythrins. *Proc. Natl. Acad. Sci. U.S.A.* **82**, 1104–1107
 70. Zhang, H., Zhang, T., Chen, K., Shen, S., Ruan, J. & Kurgan, L. (2009). On the relation between residue flexibility and local solvent accessibility in proteins. *Proteins* **76**, 617–636
 71. Buck, M., Boyd, J., Redfield, C., MacKenzie, D.A., Jeenes, D.J., Archer, D.B. & Dobson, C.M. (1995). Structural determinants of protein dynamics: analysis of ¹⁵N NMR relaxation measurements for main-chain and side-chain nuclei of hen egg white lysozyme. *Biochemistry* **34**, 4041–4055
 72. Halle, B. (2002). Flexibility and packing in proteins. *Proc. Natl. Acad. Sci. U.S.A.* **99**, 1274–1279
 73. Zhang, F. & Brüschweiler, R. (2002). Contact model for the prediction of NMR N-H order parameters in globular proteins. *J. Am. Chem. Soc* **124**, 12654–12655
 74. Marsh, J.A., Dancheck, B., Ragusa, M.J., Allaire, M., Forman-Kay, J.D. & Peti, W. (2010). Structural diversity in free and bound states of intrinsically disordered protein phosphatase 1 regulators. *Structure* **18**, 1094–1103
 75. Schlessinger, A. & Rost, B. (2005). Protein flexibility and rigidity predicted from sequence. *Proteins* **61**, 115–126
 76. Vihinen, M., Torkkila, E. & Riikonen, P. (1994). Accuracy of protein flexibility predictions. *Proteins* **19**, 141–149
 77. Fuxreiter, M. (2012). Fuzziness: linking regulation to protein dynamics. *Mol Biosyst* **8**, 168–177
 78. Collaborative Computational Project, Number 4 (1994). The CCP4 suite: programs for protein crystallography. *Acta Crystallogr. D Biol. Crystallogr* **50**, 760–763
 79. Ulrich, E.L., Akutsu, H., Doreleijers, J.F., Harano, Y., Ioannidis, Y.E., Lin, J., Livny, M., Mading, S., Maziuk, D., Miller, Z., Nakatani, E., Schulte, C.F., Tolmie, D.E., Kent Wenger, R., Yao, H. & Markley, J.L. (2007). BioMagResBank. *Nucleic Acids Res* **36**, D402–D408

Figures

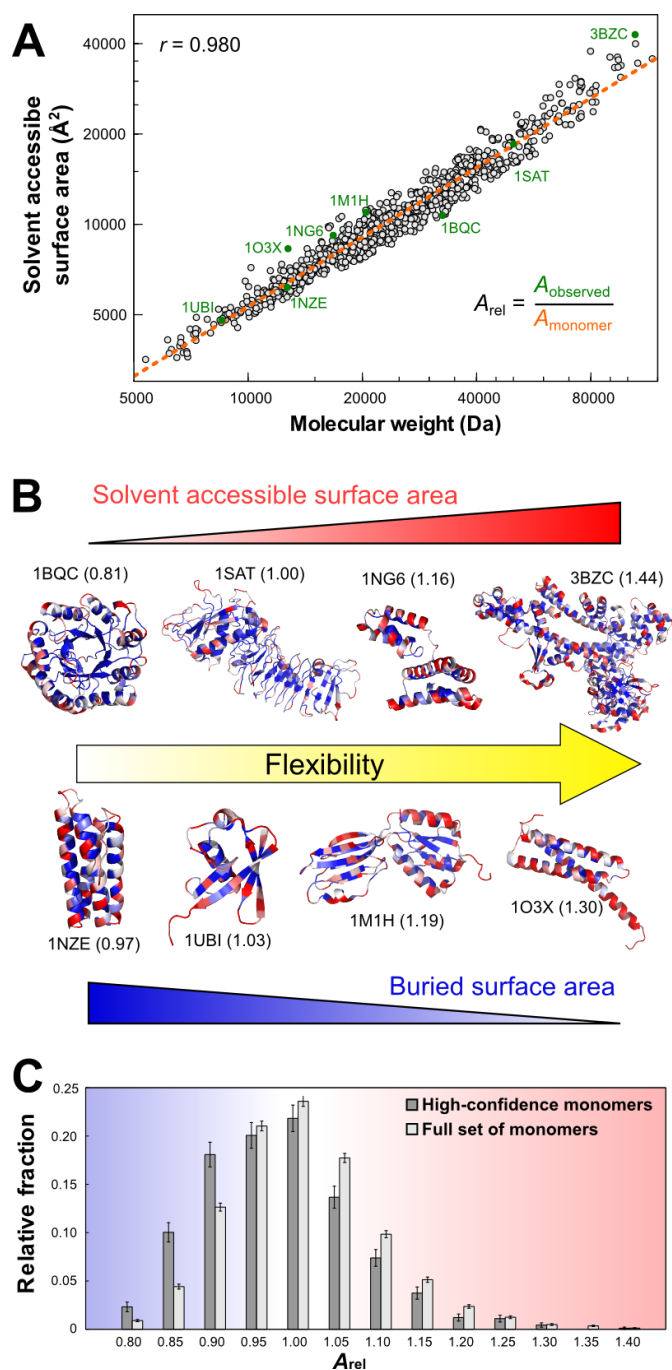


Figure 1. Relative solvent accessible surface area (A_{rel}) values of monomeric proteins. (A) Comparison of molecular weight and solvent accessible surface area values calculated from 907 non-redundant high-confidence folded, monomeric crystal structures. (B) Crystal structures of monomers of varying A_{rel} (given in brackets), with buried residues coloured blue and solvent exposed residues coloured red. These proteins are highlighted in green in panel (A). (C) Distributions of A_{rel} values for the high-confidence monomers and the full set of 6565 non-redundant monomeric crystal structures. Error bars represent the standard error of the mean.

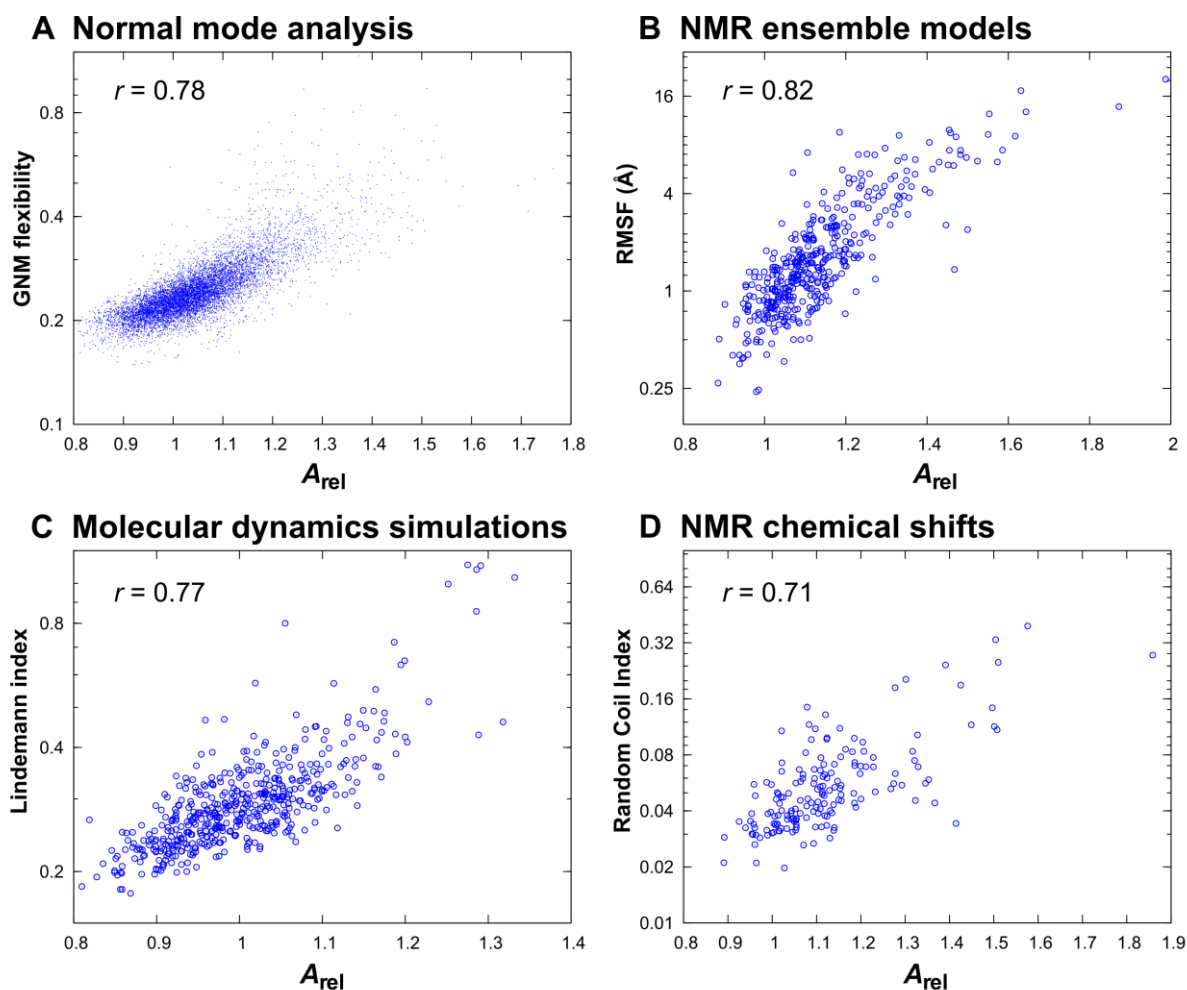


Figure 2. Comparison of monomer A_{rel} values to independent measures of intrinsic flexibility. (A) Flexibility of 6565 crystal structures calculated from Gaussian network model (GNM) normal mode analysis. (B) Root-mean-squared fluctuations (RMSF) between conformers calculated from 454 NMR models. (C) Lindemann index calculated from 491 molecular dynamics simulations in MoDEL. (D) Mean Random Coil Index (RCI) values calculated from NMR chemical shifts measured for 185 proteins. Correlations with A_{rel} are calculated with the log of the flexibility parameters, as plotted.

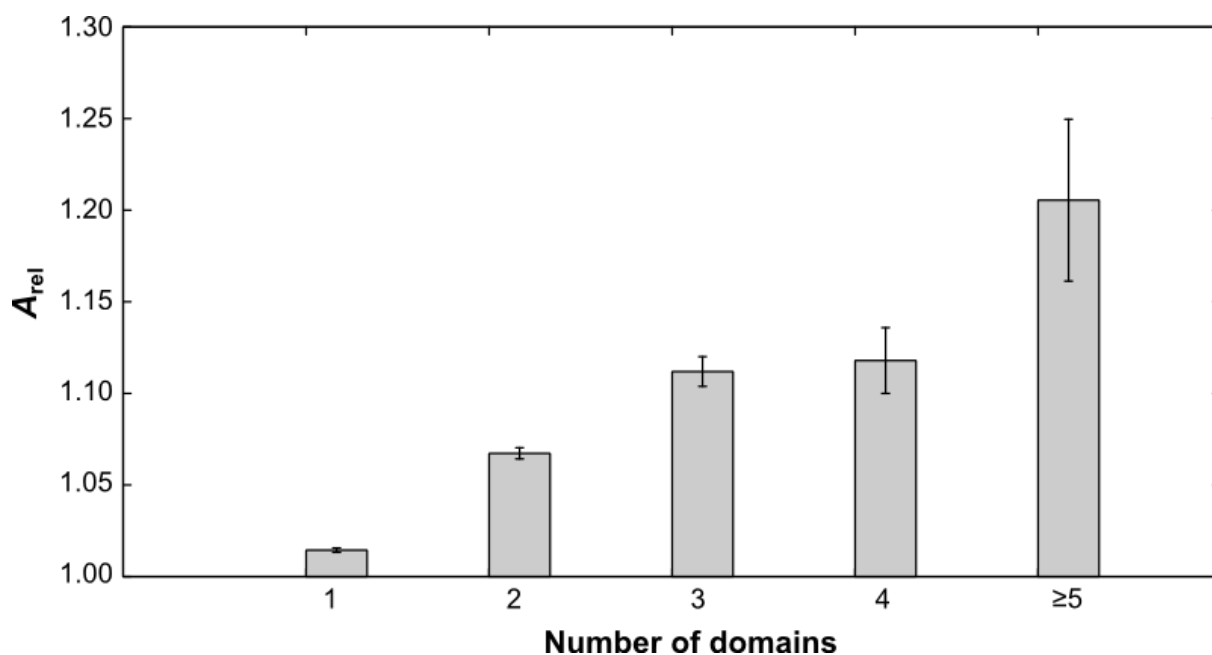


Figure 3. Association of single and multidomain proteins with intrinsic flexibility. Comparison of mean A_{rel} values from the full set of monomeric crystal structures grouped by their total number of domains. SUPERFAMILY domain assignments were used since manual SCOP assignments are not available for most proteins in the set. Error bars represent the standard error of the mean.

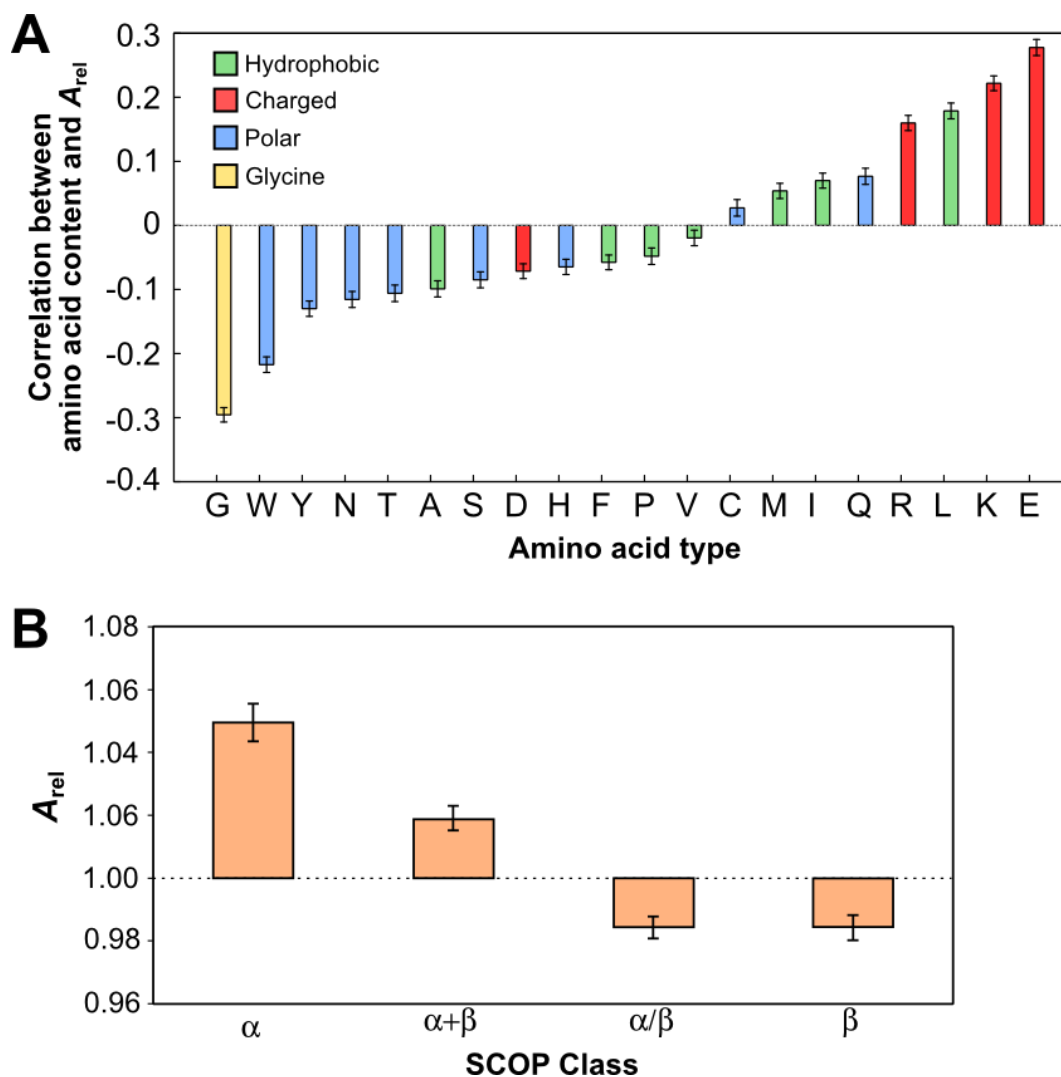


Figure 4. Sequence and secondary structure propensities associated with intrinsic protein flexibility. (A) Pearson correlation coefficients (r) between the fractional amino acid content and A_{rel} values of 6565 monomeric crystal structures. Error bars represent the standard error of the mean and were calculated from 1000 bootstrapping replicates in the same way as previously described⁵⁵. (B) Comparison of mean A_{rel} values from monomeric crystal structures grouped by SCOP class: all- α , all- β , $\alpha+\beta$ (segregated α and β regions) and α/β (β - α - β units). Only proteins with a single SCOP domain assignment were considered. All P -values were calculated with the Wilcoxon rank-sum test. Error bar represent the standard error of the mean.

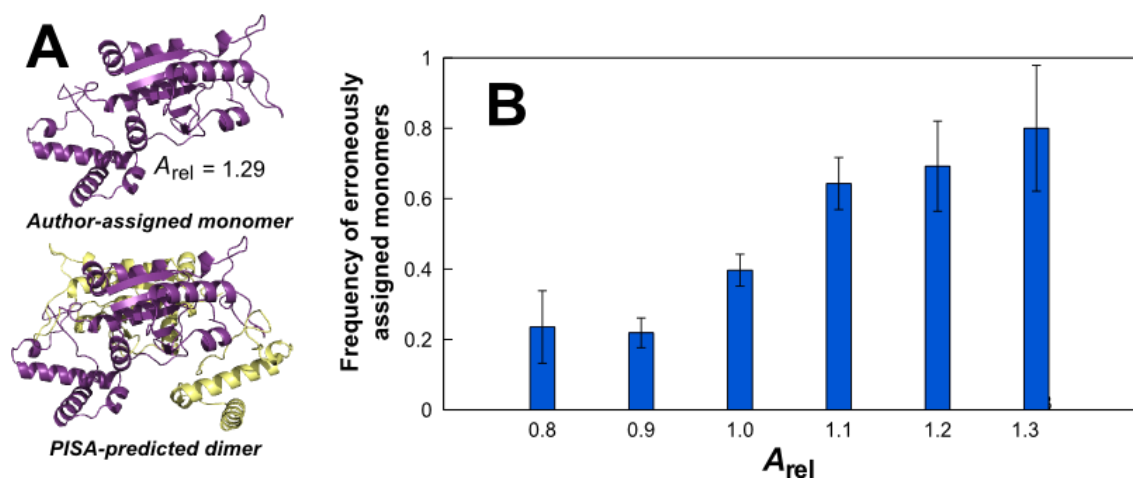


Figure 5. The relationship between intrinsic flexibility and quaternary structure assignment errors. (A) Crystal structure of the protein TrmD (PDB ID: 1P9P) which has an author-assigned monomeric biological unit (top), but which is manually annotated in PiQSi and predicted by PISA to be a homodimer (bottom). (B) Frequency of erroneous monomers for proteins with different A_{rel} values. Error bars represent the standard error of the mean.

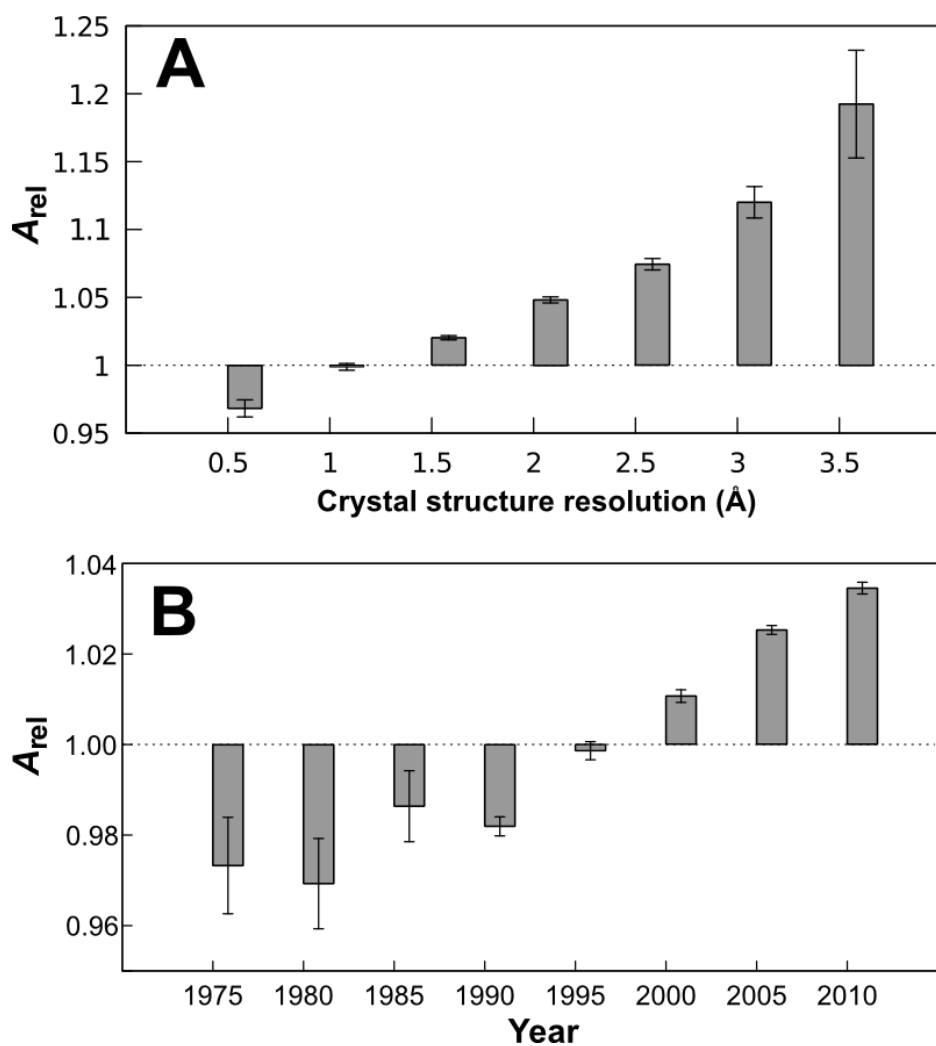


Figure 6. The relationship between intrinsic protein flexibility, crystal structure resolution and the year of structure determination. (A) Comparison of mean A_{rel} values from 6565 monomeric crystal structures of different resolutions. (B) Comparison of crystal structure A_{rel} values grouped by the year of structure determination. Error bars represent the standard error of the mean.

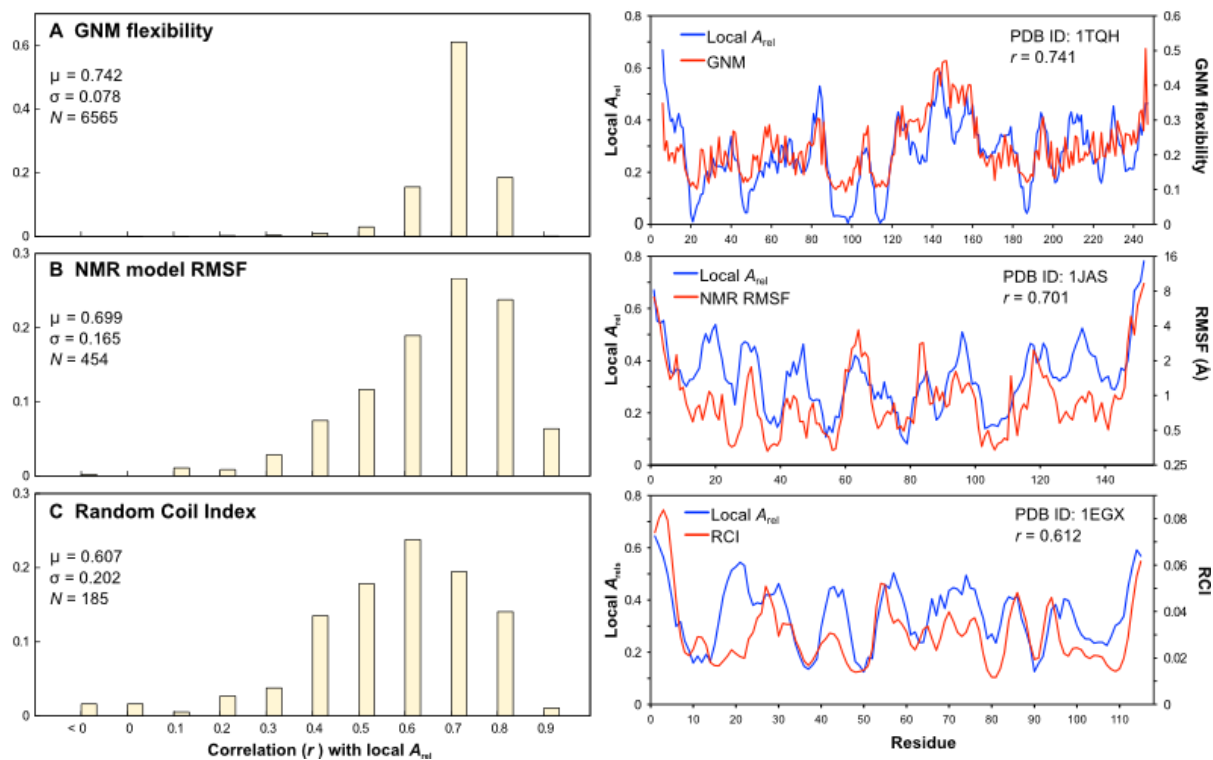


Figure 7. Comparison of local A_{rel} values to residue-specific measures of protein flexibility. The distribution between Pearson correlation coefficients (r) for individual proteins calculated between local A_{rel} values and (A) flexibility values derived from GNM normal mode analysis, (B) local RMSF values from NMR ensemble models, and (C) Random Coil Index values. On the right, a typical example for each measure is compared to local A_{rel} values. Correlations between different measures of local flexibility are provided in Table S6.

Supplementary Material

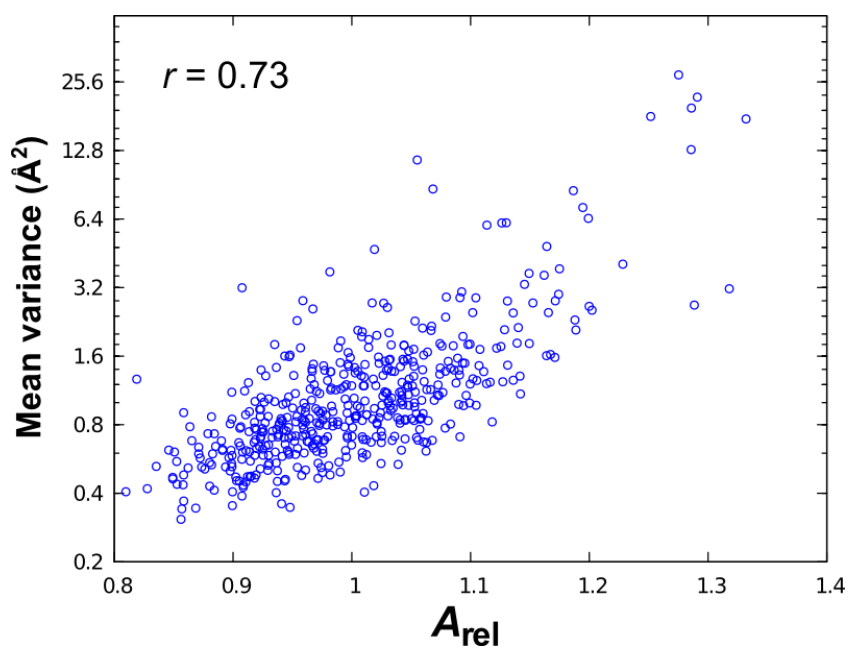


Figure S1. Comparison of A_{rel} values from 489 non-redundant monomeric crystal structures with the mean variance of $C\alpha$ atoms calculated from MoDEL molecular dynamics simulations. Note that two of the proteins used for the Lindemann index comparison do not have variance values in MoDEL, thus explaining the slightly smaller dataset.

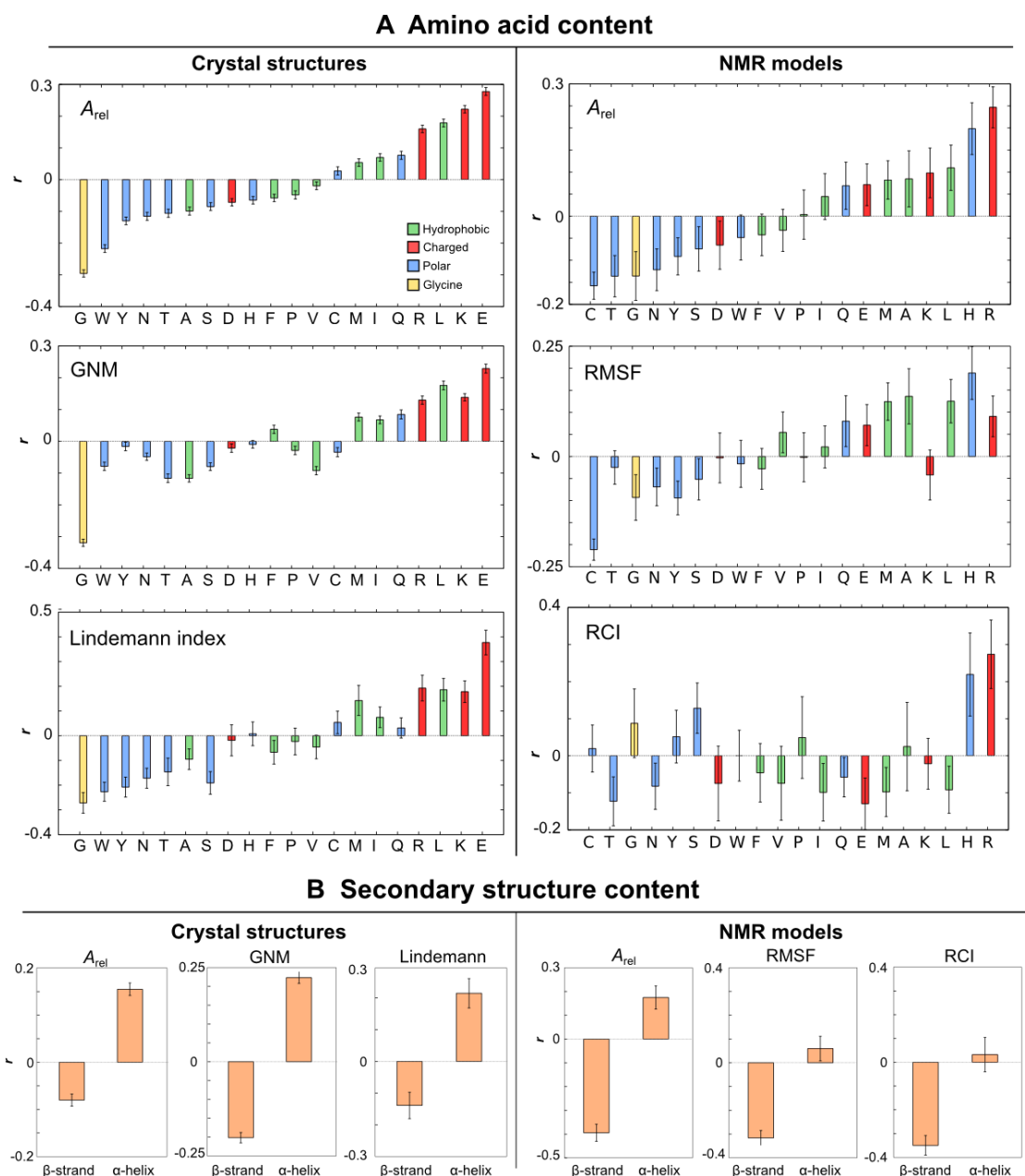


Figure S2. Correlations of different flexibility measures with amino acid and secondary structure content. (A) Exactly as in Figure 5A, except that different flexibility measures are used instead of A_{rel} . Importantly, the trend of glycine < polar < hydrophobic < charged is largely preserved across different flexibility measures. There are, however, notable differences between the crystal structures and NMR models. In particular, histidine is associated with increased flexibility, probably reflecting the fact that NMR experiments are commonly performed in slightly acidic buffers in which the histidine side chain would be charged. Although RCI shows the largest deviations from A_{rel} , note the large size of the error bars due to the much smaller dataset. (B) Similar to (A), except that fractional α -helix and β -strand content is used instead of amino acid content. Crucially, α -helices are associated with flexibility while β -strands are associated with more rigid proteins using all measures of protein flexibility. Secondary structure content was calculated from protein structures with STRIDE¹. Error bars represent standard error from 1000 bootstrapping replicates, as in Figure 4A.

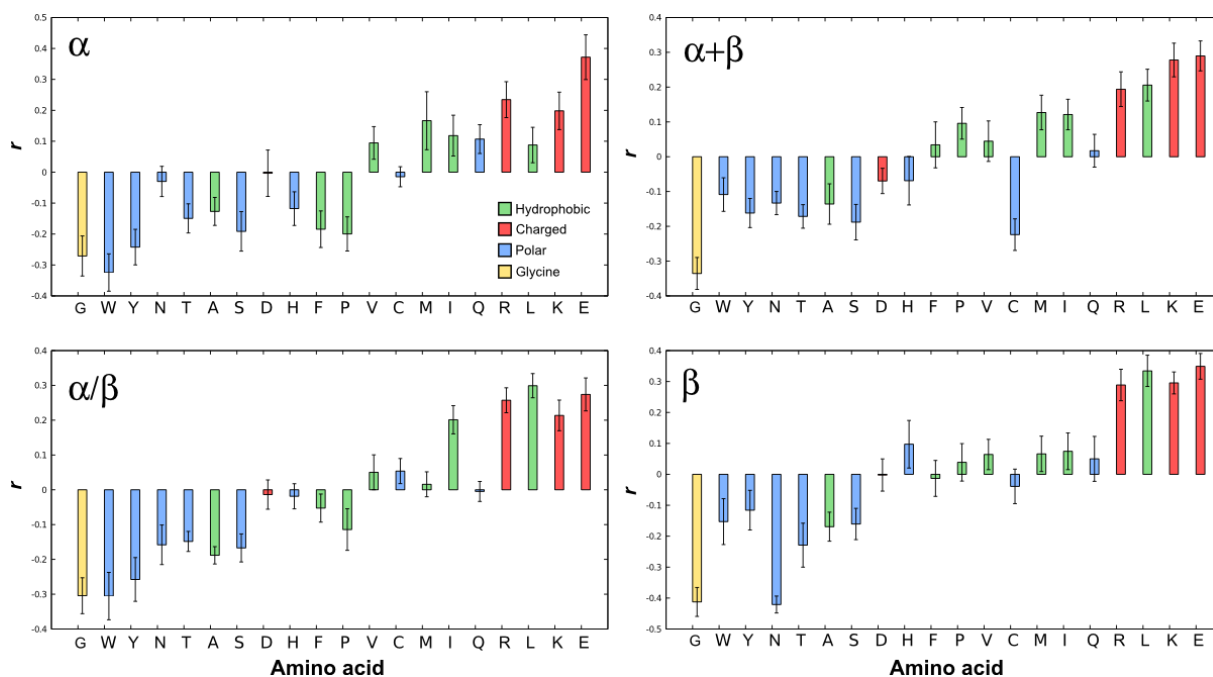


Figure S3. Correlations between fractional amino acid content and A_{rel} values for monomeric crystal structures from different SCOP classes. Note that although there are some differences, the main sequence determinants of flexibility are largely preserved across different secondary structural classes.

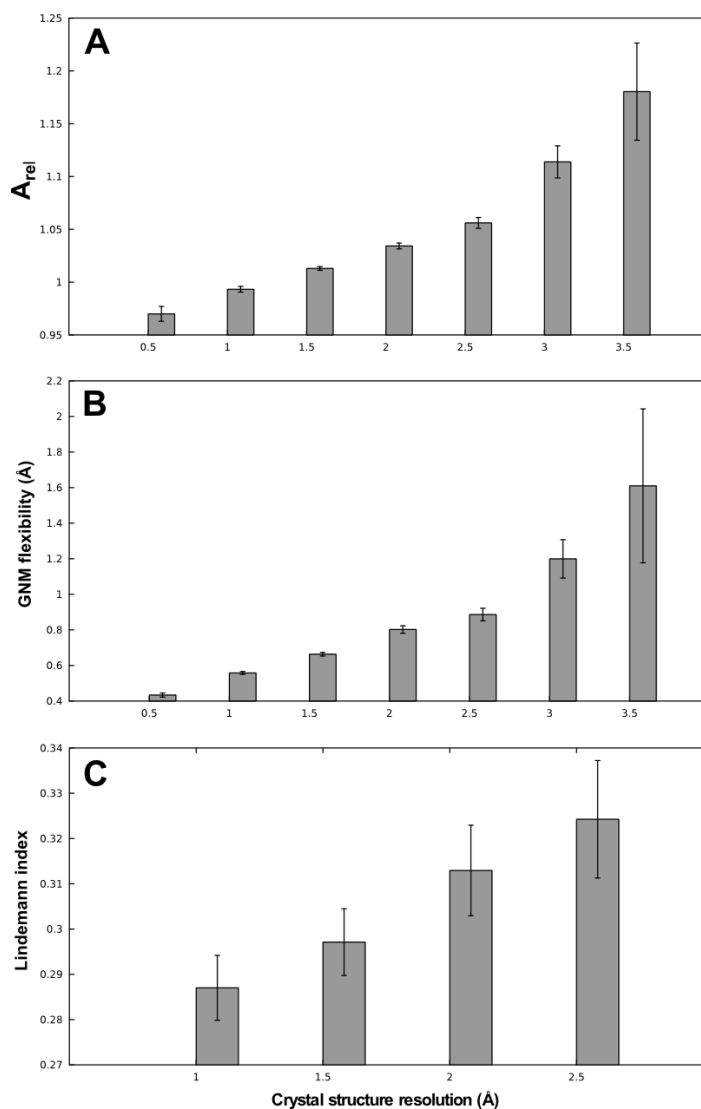


Figure S4. Comparison of different flexibility measures (A, A_{rel} ; B, GNM; C, Lindemann index) to crystal-structure resolution for monomeric structures with no missing residues. The dataset used for this analysis was filtered with the same criteria as the full dataset, except that no non-terminal disordered residues were allowed. Only bins containing at least 10 structures are shown, which accounts for the fewer bins in the smaller molecular dynamics dataset.

Table S1. Pearson correlation coefficients between independent measures of global flexibility.

| | GNM | RMSF | Lindemann | RCI |
|------------------------|------------|-------------|------------------|------------|
| A_{rel} | 0.78 | 0.82 | 0.77 | 0.71 |
| GNM | - | 0.78 | 0.69 | 0.56 |
| RMSF | - | - | 0.70 | 0.55 |
| Lindemann | - | - | - | 0.57 |

Correlations are all calculated using the log of the flexibility parameters, except A_{rel} , for consistency with the results presented in the main text.

Table S2. Pearson correlation coefficients between A_{rel} values and different measures of intrinsic flexibility, as in Figure 2, except that Equation 1 was fit using either the full set of monomers, or only single-domain proteins.

| | Full set ($A_{monomer} = 3.88M^{0.785}$) | Single-domain proteins ($A_{monomer} = 5.82M^{0.741}$) |
|------------------|--|--|
| GNM | 0.76 | 0.79 |
| RMSF | 0.81 | 0.84 |
| Lindemann | 0.78 | 0.73 |
| RCI | 0.73 | 0.67 |

Table S3. Pearson correlation coefficients between A_{rel} values and different measures of intrinsic flexibility, as in Figure 2, for single-domain and two-domain proteins.

| | Single-domain proteins | Two-domain proteins |
|------------------|-------------------------------|----------------------------|
| GNM | 0.74 | 0.76 |
| RMSF | 0.82 | 0.81 |
| Lindemann | 0.76 | 0.81 |
| RCI | 0.60 | 0.86 |

Table S4. Pearson correlation coefficients between A_{rel} values and intrinsic disorder predictions for the full set of monomeric crystal structures.

| Disorder predictor | r | P -value |
|--------------------------|-------|-------------------------|
| ESpritz ² | 0.043 | 0.0005 |
| FoldIndex ³ | 0.077 | 4×10^{-10} |
| IUPred ⁴ | 0.006 | 0.6 |
| PreDisorder ⁵ | 0.13 | $< 2.2 \times 10^{-16}$ |
| VSL2B ^{6,7} | 0.17 | $< 2.2 \times 10^{-16}$ |

The Espritz predictor was used with all default parameters and the DisProt training set (the X-ray and NMR training sets gave even weaker correlations with A_{rel}). The global FoldIndex disorder prediction score was used, but the above was inverted, as a more negative FoldIndex score indicates a stronger disorder prediction. All other disorder predictors were used with default parameters, and the average disorder predictions were averaged over all residues. Only residues observed in the crystal structures were used in the disorder predictions.

Table S5. Pearson correlation coefficients between A_{rel} values and different measures of intrinsic flexibility, as in Figure 2, for different SCOP structural classes.

| | α | $\alpha+\beta$ | α/β | β |
|------------------|----------|----------------|----------------|---------|
| GNM | 0.76 | 0.76 | 0.77 | 0.75 |
| RMSF | 0.85 | 0.83 | 0.89 | 0.88 |
| Lindemann | 0.87 | 0.71 | 0.66 | 0.59 |
| RCI | 0.46 | 0.58 | 0.66 | 0.52 |

Table S6. Mean Pearson correlation coefficients between different measures of local flexibility.

| | GNM | RMSF | RCI |
|-----------------------------|------------|-------------|------------|
| A_{rel} | 0.74 | 0.70 | 0.61 |
| GNM | - | 0.74 | 0.57 |
| RMSF | - | - | 0.61 |

Supplementary References

1. Frishman, D. & Argos, P. (1995). Knowledge-based protein secondary structure assignment. *Proteins* **23**, 566–579
2. Walsh, I., Martin, A.J.M., Di Domenico, T. & Tosatto, S.C.E. (2012). ESpritz: accurate and fast prediction of protein disorder. *Bioinformatics* **28**, 503–509
3. Prilusky, J., Felder, C.E., Zeev-Ben-Mordehai, T., Rydberg, E.H., Man, O., Beckmann, J.S., Silman, I. & Sussman, J.L. (2005). FoldIndex: a simple tool to predict whether a given protein sequence is intrinsically unfolded. *Bioinformatics* **21**, 3435–3438
4. Dosztányi, Z., Csizmók, V., Tompa, P. & Simon, I. (2005). The pairwise energy content estimated from amino acid composition discriminates between folded and intrinsically unstructured proteins. *J. Mol. Biol* **347**, 827–839
5. Deng, X., Eickholt, J. & Cheng, J. (2009). PreDisorder: ab initio sequence-based prediction of protein disordered regions. *BMC Bioinformatics* **10**, 436
6. Obradovic, Z., Peng, K., Vucetic, S., Radivojac, P. & Dunker, A.K. (2005). Exploiting heterogeneous sequence properties improves prediction of protein disorder. *Proteins* **61 Suppl 7**, 176–182
7. Peng, K., Radivojac, P., Vucetic, S., Dunker, A.K. & Obradovic, Z. (2006). Length-dependent prediction of protein intrinsic disorder. *BMC Bioinformatics* **7**, 208